Title
Cross-Polarization Dynamics in Polycrystalline Samples

Journal
Journal of Molecular Structure, 830

Authors
Taylor, Robert E
Chim, Nicholas
Dybowski, Cecil

Publication Date
2007

DOI
10.1016/j.molstruc.2006.07.06

Peer reviewed

Cross-Polarization Dynamics in Polycrystalline Samples

R. E. Taylor[1*], Nicholas Chim[1], and C. Dybowski[2*]

[1]Department of Chemistry and Biochemistry
University of California, Los Angeles
Los Angeles, CA 90095 USA

[2]Department of Chemistry and Biochemistry
University of Delaware
Newark, DE 19716 USA

*Corresponding authors:
Email addresses: taylor@chem.ucla.edu (R. Taylor)
dybowski@udel.edu (C. Dybowski)

Abstract

We observe non-monotonic development of the ^{13}C magnetization in polycrystalline samples of glycine, sucrose, and adamantine during cross-polarization. We demonstrate, by fitting the time dependence, that the development quantitatively results from dipolar oscillations. To fit the data quantitatively requires one to assume two types of spin-diffusion behavior.

Key Words:
Glycine, sucrose, adamantane, cross-polarization, depolarization, dynamics, variable contact, spin diffusion

Introduction

The combination [1] of cross-polarization (CP) enhancement [2] of rare-spin nuclei by magnetic contact with abundant nuclei and magic-angle spinning (MAS) [3-5] is one of the most commonly performed solid-state nuclear magnetic resonance (NMR) experiments. This experiment circumvents the sensitivity challenge arising from the small magnetogyric ratio, low natural abundance, and typically long spin-lattice relaxation times of most rare-spin nuclei. The efficacy of polarization transfer varies from site to site and with offset. As a result, relative quantitation is difficult [6-16].

The usual description of the cross-polarization process is a thermodynamic analysis [11] that gives an exponential rise of the magnetization followed by exponential damping due to relaxation. Limitations of this classic description were evident when transient oscillations were observed in the build-up of ^{13}C magnetization in a single crystal of ferrocene [17]. Subsequently, examples of complex behavior have been reported in polycrystalline powders [6], and even for transfer under adiabatic demagnetization [18, 19]. However, the complex behavior reported for cross-polarization transfer in polycrystalline powders has not been described in terms of non-monotonic behavior. In the original paper on polarization transfer [9], it was noted that the "bottleneck due to spin diffusion" prevents the abundant proton-spin system from being described by a single temperature during the early stage of transfer, implying that the thermodynamic theory is not applicable, at least for very short contacts. The deviations from first-order behavior observed in all these cases are similar to, but are to be distinguished from, effects in Lee-Goldberg cross-polarization, in which ^{1}H-^{13}C spin-pair interactions are predominantly responsible for polarization transfer, while proton homonuclear spin diffusion is limited [20, 21].

More detailed theoretical descriptions of the polarization-transfer process have been given [16, 22]. While the subject of non-monotonic behavior of the rare-spin magnetization has been raised, in each case the discussion was limited. For example, to avoid the difficulties of the spin-temperature approach in describing polarization transfer, Marica and Snider [16] derived exact expressions for polarization transfer between an isolated pair of spin-½ particles based on the quantum Liouville equation under both static and MAS conditions, including powder-average results, but without including spin relaxation and spin diffusion in their calculations. The results predict non-monotonic behavior, but the lack of inclusion of spin diffusion limits the practical applicability of their results to isolated spin pairs. A theoretical description of cross polarization between a spin-½ nucleus (S) and a system of *N* interacting spins-½ has also been given by Marks and Vega [22]. While discussing cross polarization in nonspinning samples, they noted that "when the frequency line shape of the S-spin signal exhibits some dipolar structure, one can expect initial transient oscillations in the CP signal as a function of the mixing time. These oscillations can be expected in particular when the S spin is coupled to a small number of I spins and the homonuclear interaction is reduced, by dilution, molecular motion, or sample spinning."

In this paper, we carefully measure and quantitatively analyze non-monotonic behavior during short cross-polarization contacts, as well as the long-contact-time relaxation behavior, for several standard polycrystalline materials. The goal is to

characterize the transfer process and its dependence on dynamic and structural parameters for these materials.

Experimental

The NMR data were acquired with a Bruker Avance 300 spectrometer using a 4-mm (outside diameter) zirconia rotor. The ^{1}H data were acquired with a single-pulse experiment. The ^{13}C and ^{15}N CP and CP/MAS spectra were acquired using a ^{1}H $\pi/2$ pulse width of 4 μs, a data acquisition time of 65 ms, and a recycle delay five times the proton spin-lattice relaxation time. The calibration of the Hartmann-Hahn match was experimentally established by adjusting relative powers to maximize the amplitude of the ^{13}C CP signal of a static adamantane sample. The contact times were varied from 10 μs to 35 ms. The three pulse sequences used for data acquisition are shown in Figure 1. The sample spin rates were varied from zero (*i.e.* a static sample) to 15 kHz.

NMR data were acquired for the α- and γ-polymorphs of glycine, as well as for sucrose and adamantane. The glycine samples were characterized by infrared spectroscopy, x-ray diffraction, and NMR spectroscopy to specify the polymorphic structure [23]. Amine-deuterated γ-glycine was synthesized by repeated dissolution in 99% D_2O, followed by freezing and lyophilization. Deuteration of the amine group was confirmed by a ^{1}H CRAMPS experiment [24]. The 98% ^{15}N-labelled glycine was purchased from Cambridge Isotope Laboratories, Inc.

The Model

The coherent-transfer model [8] is derived as an extension of the theory of Mueller *et al*. [17] for single-crystal samples dominated by a single rare-spin-abundant-spin dipolar coupling. In polycrystalline samples, different dipolar couplings arise from different orientations of the local dipolar axes relative to the magnetic field. Averaging Mueller's equation over all possible crystallite orientations and including the effects of rotating-frame spin-lattice relaxation of the protons as an overall damping (assumed to be independent of orientation) gives the following equation for the rare-spin magnetization:

$$M_C(t) = M_0\left[1 - \frac{1}{2}e^{-R_1 t} - \frac{1}{2}e^{-\frac{3}{2}R_2 t}\left(\frac{1}{2}\right) \times \int_{-\pi/2}^{\pi/2} \cos\left(\frac{b_0}{2}\left(3\cos^2\vartheta - 1\right)t\right)\sin\vartheta\, d\vartheta\right] e^{-t/T_{1\rho H}} \quad (1)$$

where R_i are proton spin-diffusion rate constants (*vide infra*), b_0 is the magnitude of the carbon-proton dipolar coupling

$$b_0 = \left(\frac{\gamma_H \gamma_C h}{2\pi r_{CH}^3}\right), \quad (2)$$

γ_i is the magnetogyric ratio of nucleus i, h is Planck's constant, and r_{CH} is the nearest proton-carbon internuclear distance. Equation (1) technically applies only to static samples; however, experience shows that it reasonably approximates the situation in a

spinning sample. Equation (1) also allows for the possibility that there are two different spin-diffusion rates for the two different terms.

We have also considered depolarization experiments of the type described by Xiaoling *et al.* [25]. The extension of the ideas behind equation (1) for polycrystalline materials leads to the following equation for the rare-spin magnetization after depolarization for a time *t*:

$$M_C(t) = \frac{M_0}{2}\left[e^{-R_1 t} + e^{-\frac{3}{2}R_2 t}\left(\frac{1}{2}\right) \times \int_{-\pi/2}^{\pi/2} \cos\left(\frac{b_0}{2}\left(3\cos^2\vartheta - 1\right)t\right)\sin\vartheta d\vartheta \right] e^{-t/T_{1\rho H}} \qquad (3)$$

The model proposed here reproduces non-monotonic behavior in polycrystalline samples in which the "enormous destructive interference in a powder sample" [16] fails to provide a simple monotonic increase in the CP signal at short contact times. This results from the interplay of a strong heteronuclear interaction and spin diffusion within the abundant spin system. This situation can arise under MAS even when the usual rare-spin line shape shows no discernable dipolar structure.

Results and Discussion

An example of the limitations of the thermodynamic model in predicting the details of experimental polarization transfer is illustrated in Figures 2 and 3. The variable-contact-time data from a ^{1}H - ^{13}C CP/MAS experiment, acquired with the pulse sequence of Figure 1a, are shown for both the carboxyl and methylene resonances of polycrystalline α-glycine spinning at 5 kHz. The solid lines represent the exponential-rise-exponential-decay that results from the classic thermodynamic description. While the fit of the thermodynamic model to the carboxyl data is reasonable, there is a rather poor fit of the same model to the methylene data. An expansion of the early behavior [bottom panel of Figure 3] shows that the increase in the ^{13}C methylene intensity is not monotonic in contact time. In particular, around 80 μs the intensity is either almost constant or decreasing. The polycrystallinity of this α-glycine sample is evident from the spectrum of Figure 4, taken under static conditions.

The application of equation (1) to the cross-polarization of a methylene carbon in α-glycine is shown in Figure 5, with an expansion of the data for short contact times shown in the lower plot. The explicit inclusion of spin diffusion and variable dipolar coupling produces a much better fit in the short-contact-time regime, as can be seen by comparison to Figure 3.

The fit of equation (1) to the variable-contact data for the methylene resonance of α-glycine uses two spin-diffusion rate constants. To be consistent with the theory of Mueller *et al.* [17], the spin-diffusion constants in the two terms in equations (1) and (3) should, in principle, be identical. However, dipolar interactions responsible for the spin diffusion are affected by both internuclear distances and motion within (segmental motion) and of the molecules (as in the case of adamantane). Our empirical results show it is almost always necessary to model the experimental data with two spin-diffusion time constants. In general, the best fit occurs for a ratio R_2/R_1 of about 3. This observation

indicates there are at least two types of spin diffusion affecting the transfer process, one relatively fast and another that is slower.

Such observations are not unique to the present results. Brus *et al.* report evidence of non-uniform proton homonuclear spin diffusion within rigid organic solids [26]. In their 2D CRAMPS experiment to study the influence of local molecular motions on proton spin-exchange in α-glycine, the polarization transfer between the nonequivalent methylene protons yielded a spin diffusion coefficient of 0.77 $nm^2\ ms^{-1}$ while polarization transfer between the methylene protons and the $-NH_3^+$ protons was 0.21-0.24 $nm^2\ ms^{-1}$. This factor of three decrease in the proton spin-diffusion coefficient arises primarily from the rotation of the hydrogen-bonded amino groups rather than from the increased internuclear distance [26-28]. Either spin-diffusion process is fast compared to spin-lattice relaxation processes.

Non-monotonic polarization-transfer behavior is not limited to α-glycine. It is also observed for the methylene resonance of γ-glycine, as shown in Figure 6. The crystal packing is different for the α- and γ-polymorphs [29-33], which results in distinctive ^1H CRAMPS spectra for the two polymorphs (Figure 7). The two methylene protons of α-glycine are shifted from each other, one being downfield as the result of a weak hydrogen bond to oxygen atoms. The neutron diffraction data of Jönsson and Kvick [31] show the methylene carbon-proton bond distances to be 0.1090 ± 0.0002 and 0.1089 ± 0.0002 nm. While this difference in length does not indicate a significant difference in bonding **within** the molecule, one methylene proton does have two unusually short contacts, 0.2390 and 0.2453 nm, with two oxygens in an adjacent layer of hydrogen-bonded glycine molecules. Within the resolution of the CRAMPS experiment, the two methylene protons in the γ-polymorph are equivalent. Similar non-monotonic behavior is also observed in amine-deuterated γ-glycine. While fully protonated γ-glycine has a ^1H spin-lattice relaxation time T_1 of 4 s, deuteration of the amine group reduces the effectiveness of the amine rotation as a relaxation mechanism and lengthens the remaining methylene ^1H T_1 to 78 s [28]. Fast proton spin diffusion still occurs between the methylene protons, but the slower proton spin diffusion now proceeds intermolecularly.

It has long been known that, at low-to-moderate magnetic fields, the dipolar coupling of the ^{14}N with its quadrupole moment to neighboring ^{13}C atoms can be observed in the ^{13}C spectrum [34-36]. That this coupling to ^{14}N is not the source of non-monotonic behavior is shown in Figure 8, in which non-monotonic behavior is observed for the methylene resonance in 98% ^{15}N-labeled α-glycine.

Non-monotonic cross-polarization behavior is not unique to the polymorphs of glycine. It is, for example, also observed for a methylene resonance of sucrose (Figure 9). Such behavior is particularly prominent for resonances of methylene carbons, which typically exhibit the strongest heteronuclear dipolar interactions with protons. Methylenes have a stronger dipolar effect than methines due to the fact that there are two bonded protons. In methyl groups the heteronuclear dipolar interaction is attenuated due to rapid rotation about the three-fold axis [27].

Short-contact experiments can indeed be complementary to ^1H 2D CRAMPS studies for exploring spin-exchange in larger molecules. The indirect detection of the proton spin-exchange through observation of ^{13}C may circumvent the spectral resolution difficulties of typical ^1H linewidths of 0.5 to 3 ppm observed in most CRAMPS experiments, as demonstrated by Wang and White [37] when measuring ^1H spin diffusion

in polyisobutylene. As an example of the complementary nature of the short-contact experiments to the CRAMPS experiments, in Figure 9, the non-monotonic behavior of the sucrose methylene allows one to infer the existence of multiple couplings that could probably not be resolved in a CRAMPS spectrum of the same material.

The measurement of local ^{1}H spin-diffusion coefficients, especially through indirect detection of the proton spin exchange, is an active area of investigation [38]. The challenges include distinguishing between intra- and intermolecular spin diffusion, variation of spin-diffusion coefficients (including measurements on different length scales, in the presence of spin-locking or decoupling, and the effect of magic angle spinning), methods to measure the diffusion coefficients, and systems where non-uniform behavior is observed. Specifically, as discussed by Chen and Schmidt-Rohr [38], the analysis of intramolecular spin diffusion is "particularly useful for systems with significant segmental motions, which partially average the homonuclear dipolar interactions", as in the case of glycine.

^{13}C CP/MAS depolarization results [25] have been reported for several compounds, including polycrystalline glycine. The depolarization data presented here for the methylenes of α-glycine (Figure 10) fit equation (3), which uses two spin-diffusion rate constants and accounts for the variation of dipolar coupling with orientation and segmental motion, with parameters identical to those for the variable contact cross-polarization of this material. The fit reproduces most characteristics of the observed depolarization results.

In the variable-contact cross-polarization and depolarization experiments, similar behaviors are observed at different sample rotation rates. In the static and slow-spinning regimes, there is a fast energy exchange between the protonated ^{13}C and its directly bonded proton(s) and then a slower approach to quasi-equilibrium via energy exchange with the whole ^{1}H spin system. For spin rates up to 5 kHz, there is a lengthening of the plateau or non-monotonic behavior prior to the onset of spin diffusion. However, in the "fast" spinning regime, the results indicate that spin diffusion is much less effective, with both rate constants being much smaller than for the slow-spinning regime. As shown in Figure 11 for the variable contact data of the methylene resonance of α-glycine obtained at a spin rate of 13 kHz, the observed non-monotonic behavior corresponds to the period (ca. 77 μs and multiples thereof) of the sample spinning. Equation (1) simply cannot reproduce this complex behavior, as the model was developed for the static case. For static and slow-spinning data (i.e., Figures 5, 6, and 10), the models for polarization transfer and depolarization provide a reasonable fit to both the breadth and the intensity of the non-monotonic behavior. However, in Figure 11, the model does not reproduce the intensity and width of the sharp fall and rise corresponding to the spin rate modulation. This shape of the spinning modulation is reminiscent of the very sharp rise and fall observed for each rotational echo [39]. As the static model contains no mechanism for reproducing the spin rate modulation, the limitation of the model at high spin rates is understandable.

The transition from a regime of fast energy exchange and slower spin diffusion to a regime in which transfer is modulated by the spin rate is a result of the averaging of the dipolar interaction, as can be seen by the effects in the ^{1}H spectra as a function of the spin rate, shown in Figure 12. The ^{1}H homonuclear dipolar interaction is homogenous. Only at spin rates of 7 kHz and higher are there signs of MAS averaging affecting the

homonuclear dipolar interaction. In other words, a "slow" MAS rate is one small compared to the natural ^{1}H line width, while a "fast" MAS rate is able to narrow the ^{1}H resonance.

The effect of sample spin rate can also be seen in the polarization transfer to the carboxyl and methylene resonances of α-glycine for a fixed contact time of 3 ms while varying the Hartmann-Hahn match, as shown in Figure 13. The two resonances represent opposite extremes with regard to the heteronuclear dipolar coupling to the protons. The weakly coupled non-protonated carboxyl is more sensitive to MAS averaging than the very strongly coupled methylene.

The depolarization experiments of Xiaoling *et al*. [25] were performed at a slow sample spin rate with the initial ^{13}C magnetization generated through cross-polarization from the protons. The data presented here reproduce their results. However, in the fast-spinning regime, a short t_i, meant to allow dephasing of the proton magnetization prior to the ^{13}C depolarization, on the order of one ms proved insufficient. At such values of t_i with high sample spin rates, further polarization transfer from the protons to the methylene and carboxyl in glycine is still observed. Increasing the time for destruction of the ^{1}H magnetization to 20 ms also proved insufficient for fast sample spinning. Such a result is to be expected because the ^{1}H resonance is narrowed (lengthening the apparent T_2), as shown in Figure 12. As a result it was necessary to modify the depolarization experiment with fast sample spinning to create the ^{13}C magnetization with a single ^{13}C $\pi/2$ pulse using the pulse sequence shown in Figure 1c.

One of the classic examples of ^{13}C cross-polarization dynamics is that for adamantane [11]. The intensities as a function of contact time of both the methylene and methine resonances in a static sample of adamantane exhibit identical behavior. This is consistent with the random isotropic motion of the adamantane molecule in the plastic crystal at ambient temperature averaging out the intramolecular dipolar interaction, so that the intermolecular dipolar interaction provides the cross polarization. However, a detailed examination of the early polarization transfer to the carbon resonances in adamantane also shows the characteristically non-thermodynamic behavior of a fast transfer from the directly bonded proton(s) followed by a slower transfer limited by spin diffusion, as shown for the downfield methylene resonance in Figure 14.

Conclusions

The short-contact data for several molecular compounds containing methylene groups show systematic deviations from the predictions of the thermodynamic model in the time regime prior to the establishment of a quasi-equilibrium in the spin system. When the dipolar interactions are sufficiently strong, even polycrystalline materials show oscillatory behavior analogous to those in single-crystal materials. The sample spin rate affects the non-monotonic behavior. In the static and "slow" sample spinning regimes, polarization transfer is characterized by a rapid rise due to the strong heteronuclear dipolar coupling of directly bonded protons followed by a slower approach to quasi-equilibrium via energy exchange with the whole ^{1}H spin system through spin diffusion. In the "fast" spinning regime, spin diffusion is slow, as a result of averaging of the dipolar coupling.

The Hartmann-Hahn match versus the sample spin rate depends strongly on the strength of the dipolar coupling. In glycine, the strongly heteronculear dipolar-coupled methylene resonance shows less interference from MAS averaging than does the weakly heteronuclear dipolar-coupled carbonyl resonance as a function of the spin rate.

Acknowledgment

This material is based upon work supported by the National Science Foundation under Equipment Grant # DMR-9975975. CD acknowledges the support of the National Science Foundation under Grant # CHE-0411790.

References

[1] J. Schaefer and E. O. Stejskal, Carbon-13 Nuclear Magnetic Resonance of Polymers Spinning at the Magic Angle. *J. Am. Chem. Soc.* 98 (1976) 1031-1032.

[2] A. Pines, M. G. Gibby, and J. S. Waugh, Proton-Enhanced Nuclear Induction Spectroscopy. A Method for High Resolution NMR of Dilute Spins in Solids. *J. Chem. Phys.* 56 (1972) 1776-1777.

[3] E. R. Andrew, A. Bradbury, and R. G. Eades, Nuclear Magnetic Resonance Spectra from a Crystal rotated at High Speed. *Nature* 182 (1958) 1659.

[4] E. R. Andrew, A. Bradbury, and R. G. Eades, Removal of Dipolar Broadening of Nuclear Magnetic Resonance Spectra of Solids by Specimen Rotation. *Nature* 183 (1959) 1802-1803.

[5] I. J. Lowe, Free Induction Decays of Rotating Solids. *Phys. Rev. Lett.* 2 (1959) 285-287.

[6] W. Kolodziejski and J. Klinowski, Kinetics of Cross-Polarization in Solid-State NMR: A Guide for Chemists. *Chem. Rev.* 102 (2002) 613-628.

[7] D. G. Rethwisch, M. A. Jacintha, and C. R. Dybowski, Quantification of ^{13}C in solids using CPMAS-DD-NMR spectroscopy. *Anal. Chim. Acta* 283 (1993) 1033-1043.

[8] J. M. Smith, C. Dybowski, and S. Bai, Kinetics of NMR spin-lock polarization transfer in crystalline glycine and spin-lattice relaxation of amino acids. *Solid State NMR* 27 (2005) 149-154.

[9] S. R. Hartmann and E. L. Hahn, Nuclear Double Resonance in the Rotating Frame. *Phys. Rev*. 128 (1962) 2042-2053.

[10] F. M. Lurie and C. P. Schlicter, Spin Temperature in Nuclear Double Resonance. *Phys. Rev*. 133 (1964) A1108-A1122.

[11] A. Pines, M. G. Gibby, and J. S. Waugh, Proton-enhanced NMR of dilute spins in solids. *J. Chem. Phys*. 59 (1973) 569-590.

[12] E. O. Stejskal, J. Schaefer, and J. S. Waugh, Magic-Angle Spinning and Polarization Transfer in Proton-Enhanced NMR. *J. Magn. Reson*. 28 (1977) 105-112.

[13] M. Sardashti and G. E. Maciel, Effects of Sample Spinning on Cross Polarization. *J. Magn. Reson*. 72 (1987) 467-474.

[14] B. H. Meier, Cross polarization under fast magic angle spinning: thermodynamical considerations. *Chem. Phys. Lett*. 188 (1992) 201-207.

[15] J.-P. Amoureux and M. Pruski, Theoretical and experimental assessment of single- and multiple-quantum cross-polarization is solid state NMR. *Mol. Phys*. 100 (2002) 1595-1613.

[16] F. Marica and R. F. Snider, An analytical formulation of CPMAS. *Solid State NMR* 23 (2003) 28-49.

[17] L. Müller, A. Kumar, T. Baumann, and R. R. Ernst, Transient Oscillations in NMR Cross-Polarization Experiments in Solids. *Phys. Rev. Lett*. 32 (1974) 1402-1406.

[18] D. A. McArthur, E. L. Hahn, and R. E. Walstedt, Rotating-Frame Nuclear-Double-Resonance Dynamics: Dipolar Fluctuation Spectrum in CaF_2. *Phys. Rev*. 188 (1969) 609-638.

[19] D. V. Lang and P. R. Moran, Rotating-Frame Double Resonance and Nuclear Cross Relaxation in LiF. *Phys. Rev. B* 1 (1970) 53-62.

[20] B.-J. van Rossum, C. P. de Groot, V. Ladizhansky, S. Vega, and H. J. M. de Groot, A Method for Measuring Heteronuclear (^{1}H-^{13}C) Distances in High Speed MAS NMR. *J. Am. Chem. Soc.* 122 (2000) 3465-3472.

[21] V. Ladizhansky and S. Vega, Polarization transfer dynamics in Lee-Goldburg cross polarization nuclear magnetic resonance experiments on rotating solids. *J. Chem. Phys.* 112 (2000) 7158-7168.

[22] D. Marks and S. Vega, A Theory for Cross-Polarization NMR of Nonspinning and Spinning Samples. *J. Magn. Reson. Series A* 118 (1996) 157-172.

[23] R. E. Taylor, ^{13}C CP/MAS: Application to Glycine. *Concepts Magn. Reson.* 22A (2004) 79-89.

[24] L. M. Ryan, R. E. Taylor, A. J. Paff, and B. C. Gerstein, An experimental study of resolution of proton chemical shifts in solids: Combined multiple pulse NMR and magic-angle spinning. *J. Chem. Phys*., 72 (1980) 508-515.

[25] W. Xiaoling, Z. Shanmin, and W. Xuewen, Two-stage feature of Hartmann-Hahn cross relaxation in magic-angle sample spinning. *Phys. Rev. B* 37 (1988) 9827-9829.

[26] J. Brus, H. Petříčková, and J. Dybal, Influence of local molecular motions on the determination of ^{1}H-^{1}H internuclear distances measured by 2D ^{1}H spin-exchange experiments. *Solid State NMR* 23 (2003) 183-197.

[27] X. Wu and K. W. Zilm, Complete Spectral Editing in CPMAS NMR. *J. Magn. Res. Series A* 102 (1993) 205-213.

[28] R. E. Taylor, N. Chim, and C. Dybowski, NMR characterization of partially deuterated γ-glycine. *J. Mol. Struct.*, XX, YYY-ZZZ (2006).

[29] R. E. Marsh, A Refinement of the Crystal Structure of Glycine. *Acta Crystallogr*. 11 (1958) 654-663.

[30] Y. Iitaka, The crystal structure of γ-glycine. *Acta Crystallogr*. 11 (1958) 225-226.

[31] P-G. Jönsson and A. Kvick, *Acta Crystallogr. B* 28 (1972) 1827-1833.

[32] L. F. Power, K. E. Turner, and F. H. Moore, The Crystal and Molecular Structure of α-Glycine by Neutron Diffraction - a Comparison. *Acta Crystallogr. B* 32 (1976) 11-16.

[33] A. Kvick, W. M. Canning, T. F. Koetzle, and G. J. B. Williams, An Experimental Study of the Influence of Temperature on a Hydrogen-Bonded System: The Crystal Structure of γ-Glycine at 83 K and 298 K by Neutron Diffraction. *Acta Crystallogr. B* 36 (1980) 115-120.

[34] M. E. Stoll, R. W. Vaughan, R. B. Saillant, and T. Cole, ^{13}C chemical shift tensor in $K_2Pt(CN)_4Br_{0.3}.3H_2O$. *J. Chem. Phys.* 61 (1974) 2896-2899.

[35] S. J. Opella, M. H. Frey, and T. A. Cross, Detection of Individual Carbon Resonances in Solid Proteins. *J. Am. Chem. Soc.* 101 (1979) 5856-5857.

[36] N. Zumbulyadis, P. M. Henrichs, and R. H. Young, Quadrupole effects in the magic-angle-spinning spectra of spin-½ nuclei. *J. Chem. Phys*. 75 (1981) 1603-1611.

[37] X. Wang and J. L. White, Intramonomer Polarization Transfer: Calibrating Spin Diffusion Coefficients in Mobile Polyolefins and Their Blends. *Macromolecules* 35 (2002) 3795-3798.

[38] Q. Chen and K. Schmidt-Rohr, Measurement of the local ^{1}H spin-diffusion coefficent in polymers. *Solid State NMR* 29 (2006) 142-152.

[39] R. E. Taylor, Setting up ^{13}C CP/MAS Experiments. *Concepts Magn. Reson.* 22A (2004) 37-49.

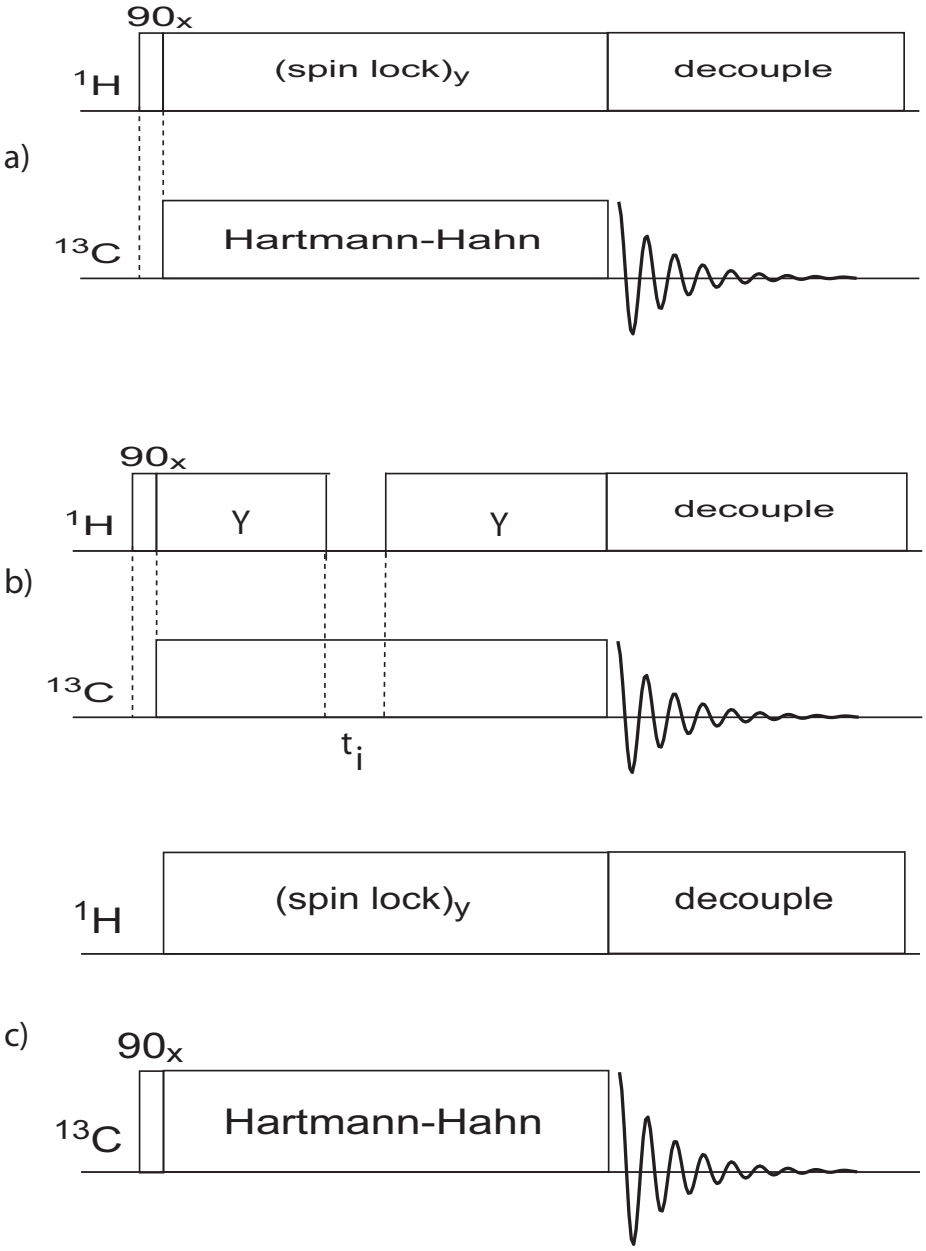

Figure 1. The pulse sequences used for ^{13}C data acquisition: a) standard single-contact cross-polarization; b) depolarization, as described in reference 25; and c) depolarization as modified to avoid long-lived ^{1}H magnetization arising in the fast MAS experiments.

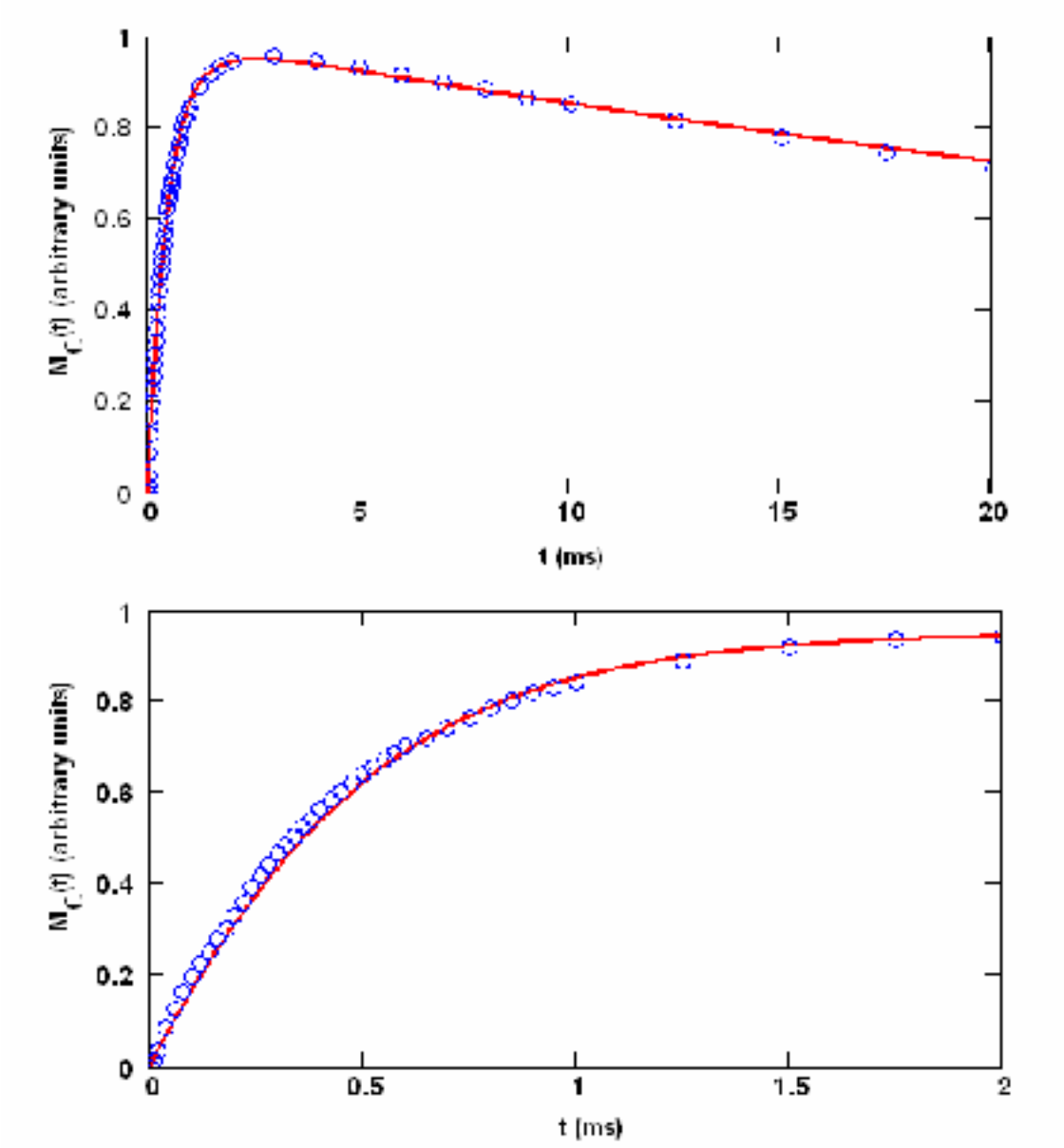

Figure 2. ^{1}H-^{13}C CP/MAS variable-contact-time data for the carboxyl carbon of α-glycine, with an expansion shown in the bottom panel. The fit in each panel is to the first-order thermodynamic model. The sample was spinning at 5 kHz.

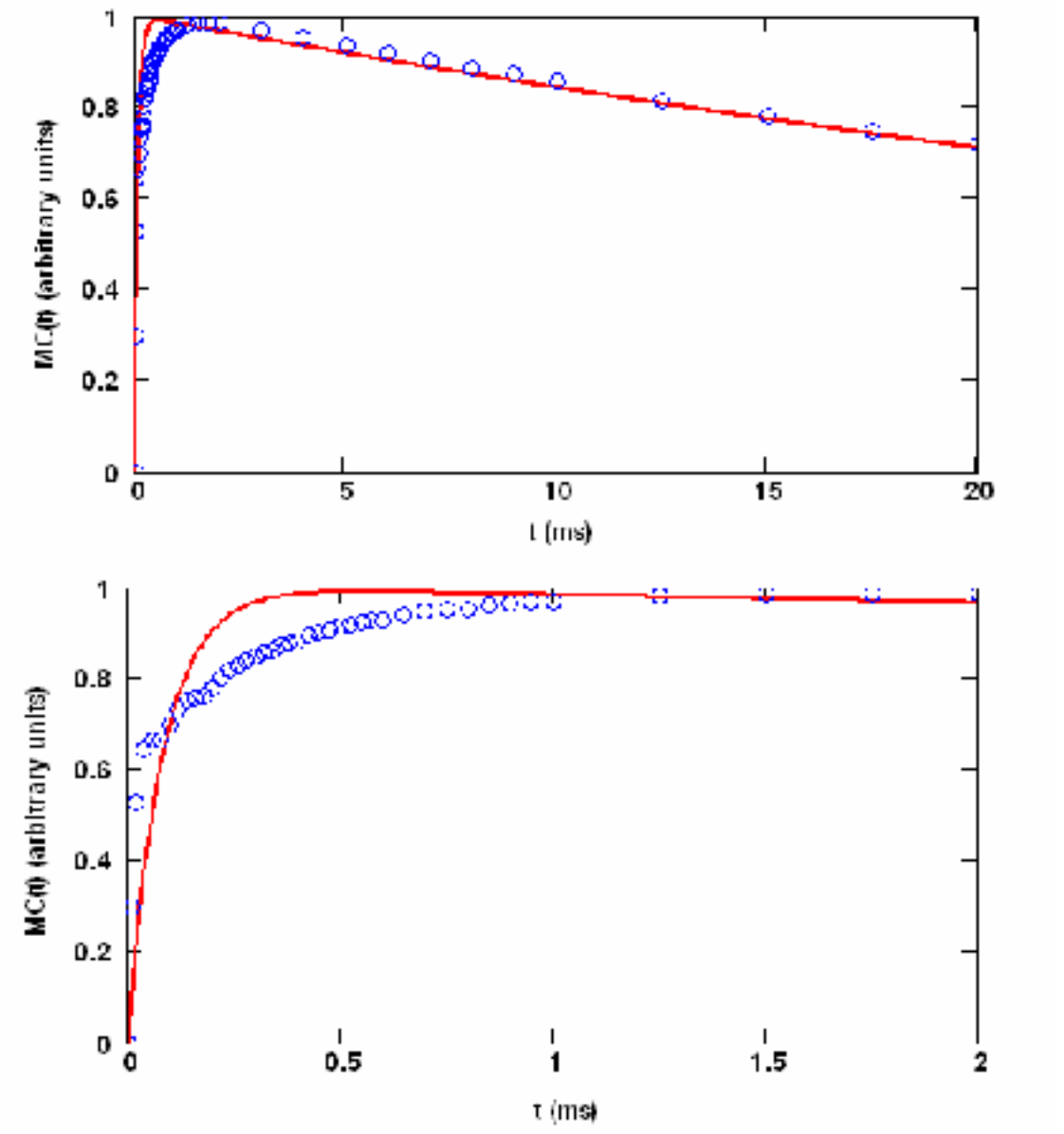

Figure 3. ^{1}H-^{13}C CP/MAS variable-contact data for the methylene carbon of α-glycine. In the bottom expanded panel, it is obvious that the data do not obey the thermodynamic model. The sample was spinning at 5 kHz.

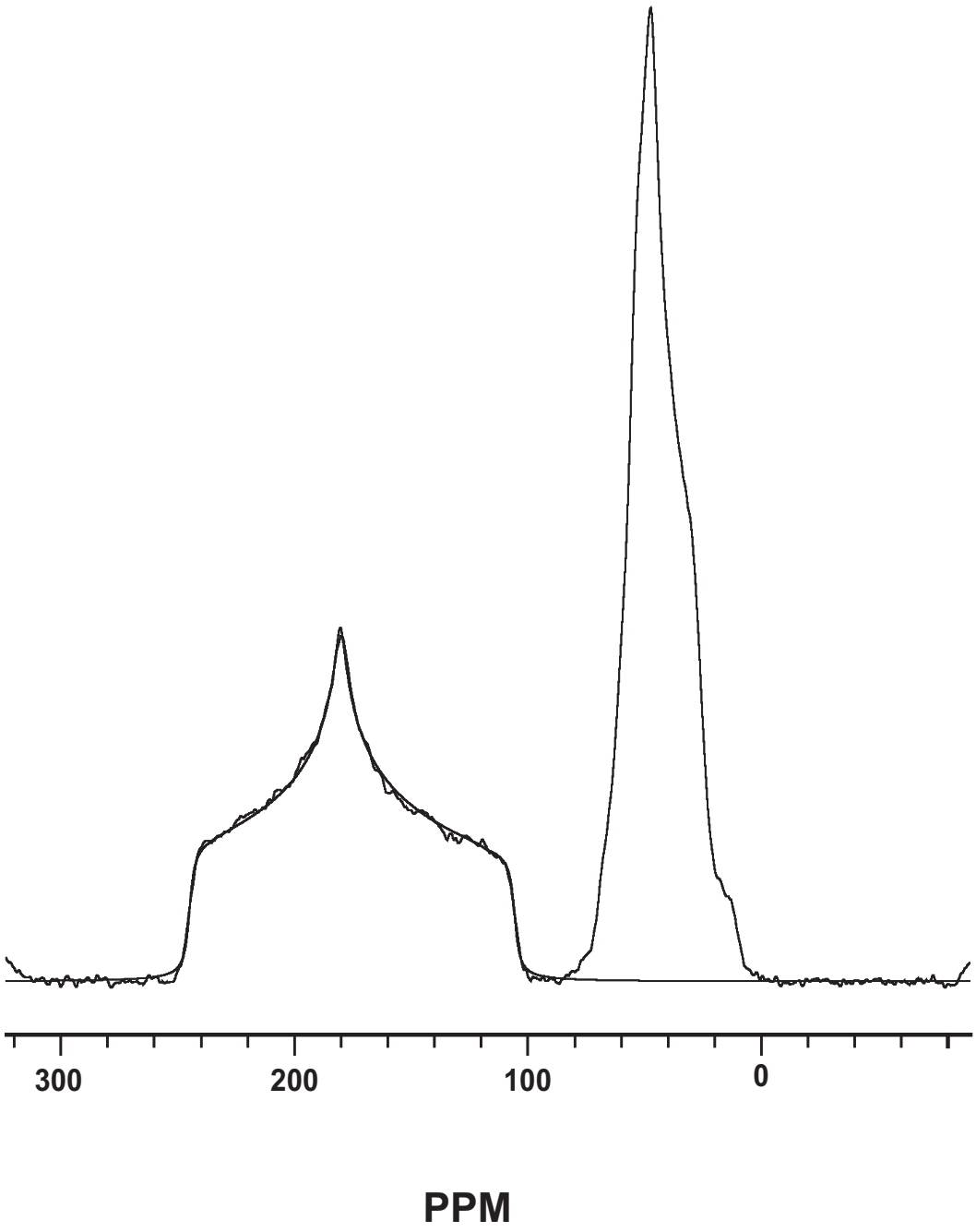

Figure 4. ^{13}C CP spectrum of a static sample of α-glycine. The carboxyl resonance shows an asymmetric chemical-shift powder pattern (fit with smooth line), while the methylene resonance shows both an axially symmetric chemical-shift powder pattern and dipolar coupling to the quadrupolar ^{14}N.

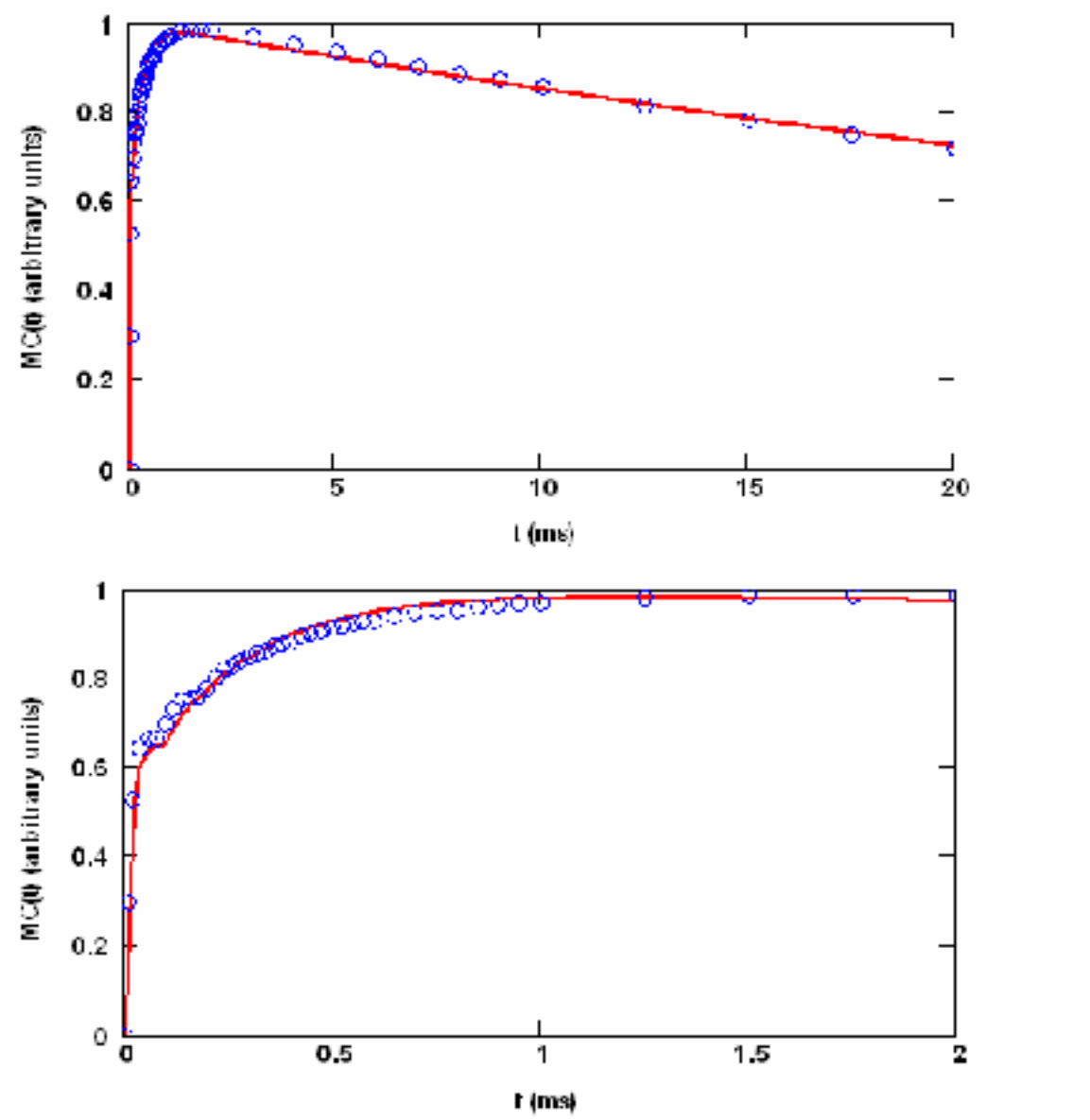

Figure 5. Fit of equation (1) to the variable-contact methylene data of α-glycine. The top figure shows the full data set. The bottom shows the early non-monotonic behavior. Comparing these results to the thermodynamic model of Figure 3, equation (1) provides a better fit to the experimental data at short contact times than the traditional thermodynamic model. The sample was spinning at 5 kHz.

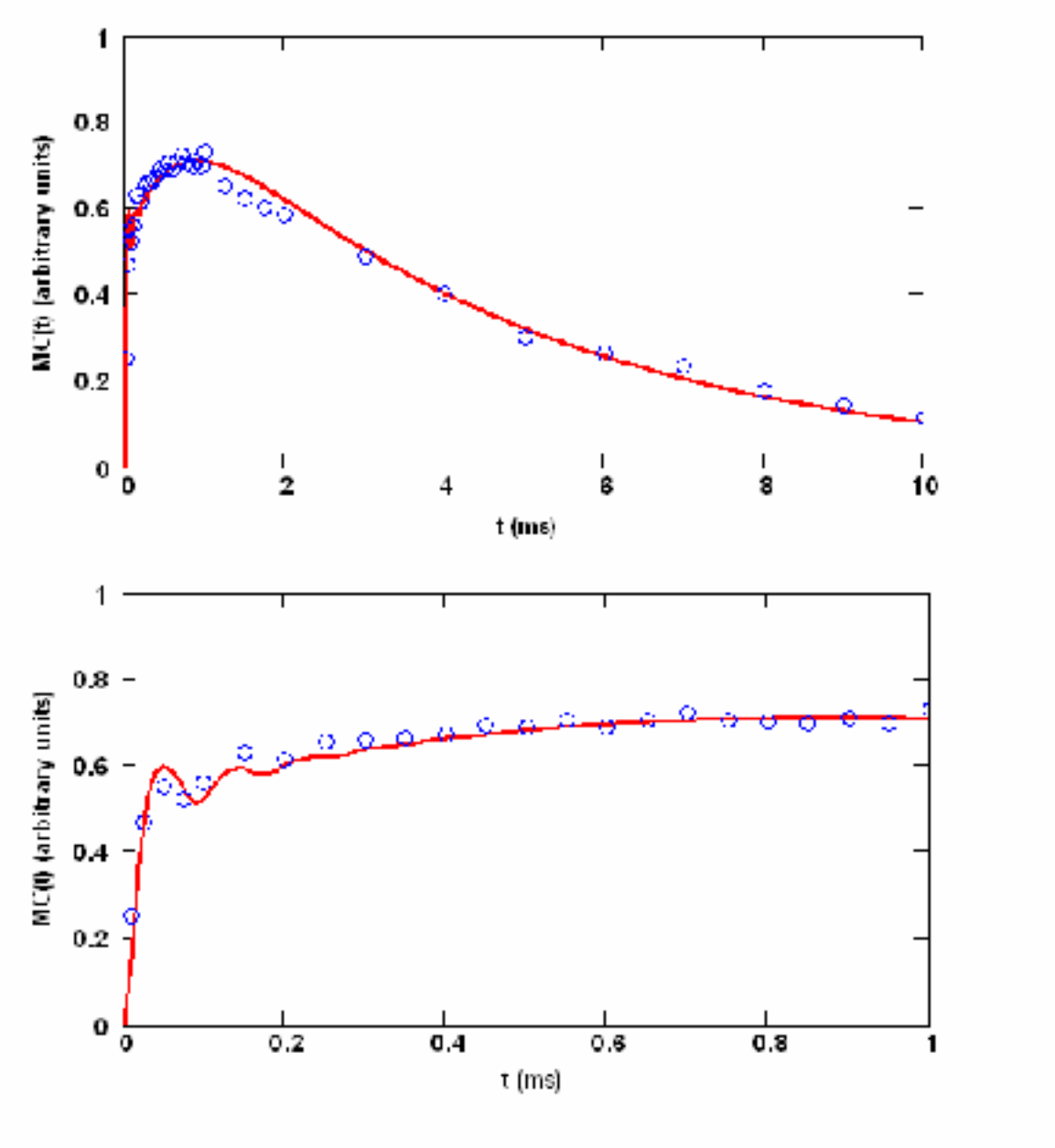

Figure 6. ^{1}H-^{13}C CP/MAS variable-contact data for the methylene resonance of polycrystalline γ-glycine. The bottom panel is an expansion of the first millisecond. The sample was spinning at 5 kHz.

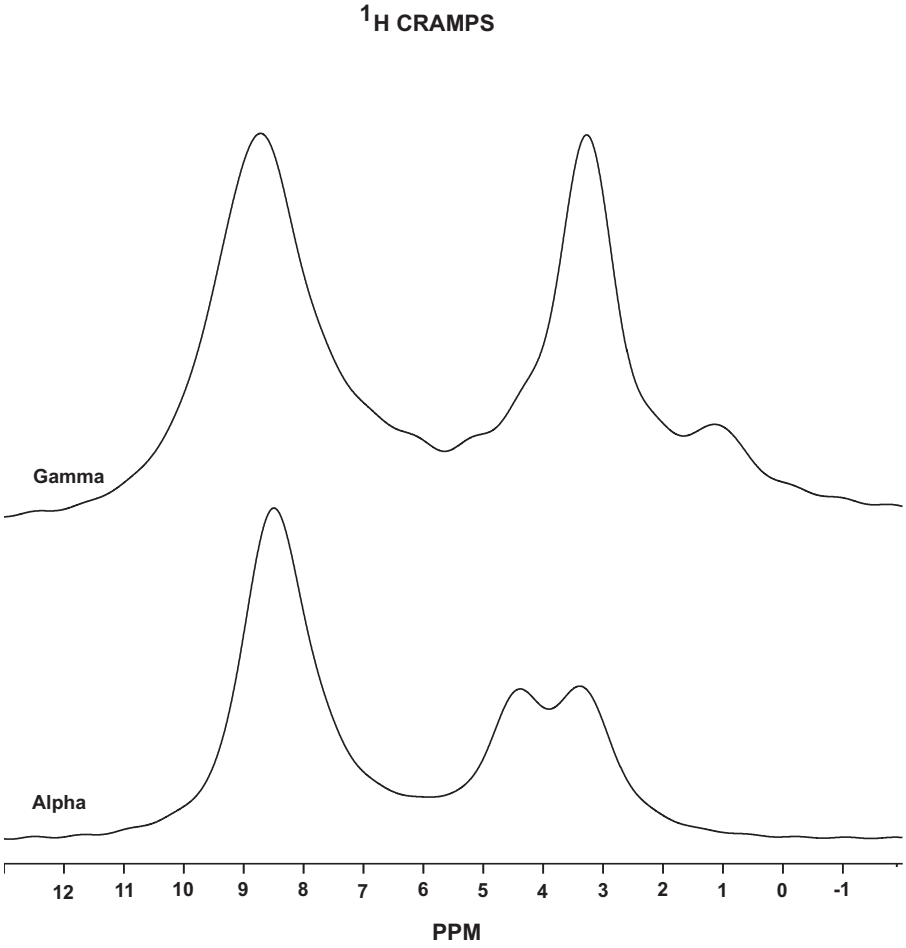

Figure 7. ^{1}H CRAMPS spectra of γ-glycine (top) and α-glycine (bottom).

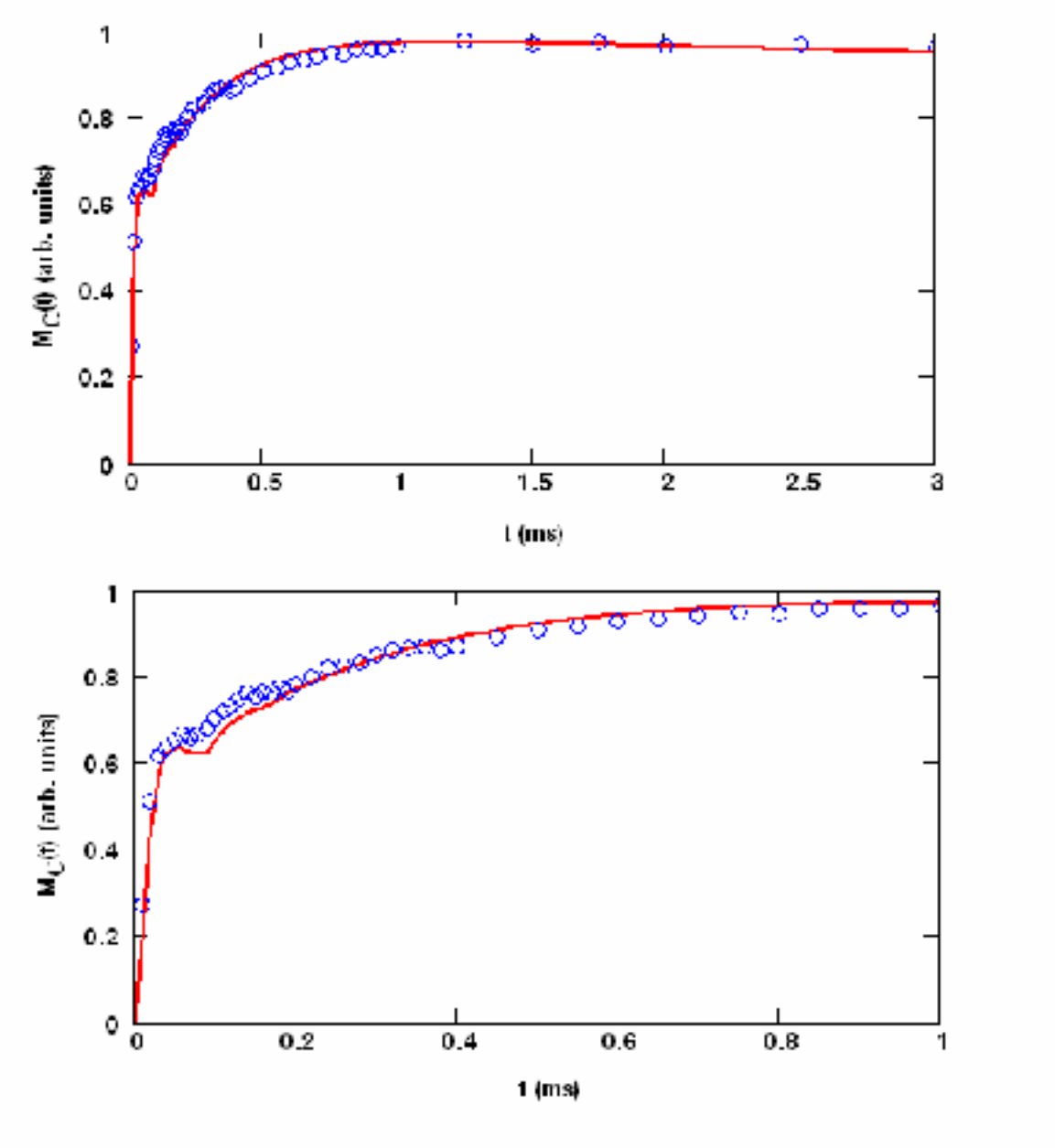

Figure 8. ^{1}H-^{13}C CP/MAS variable-contact data for the methylene resonance of polycrystalline 98% ^{15}N-enriched α-glycine. The bottom panel shows the early part of this curve. The sample was spinning at 5 kHz.

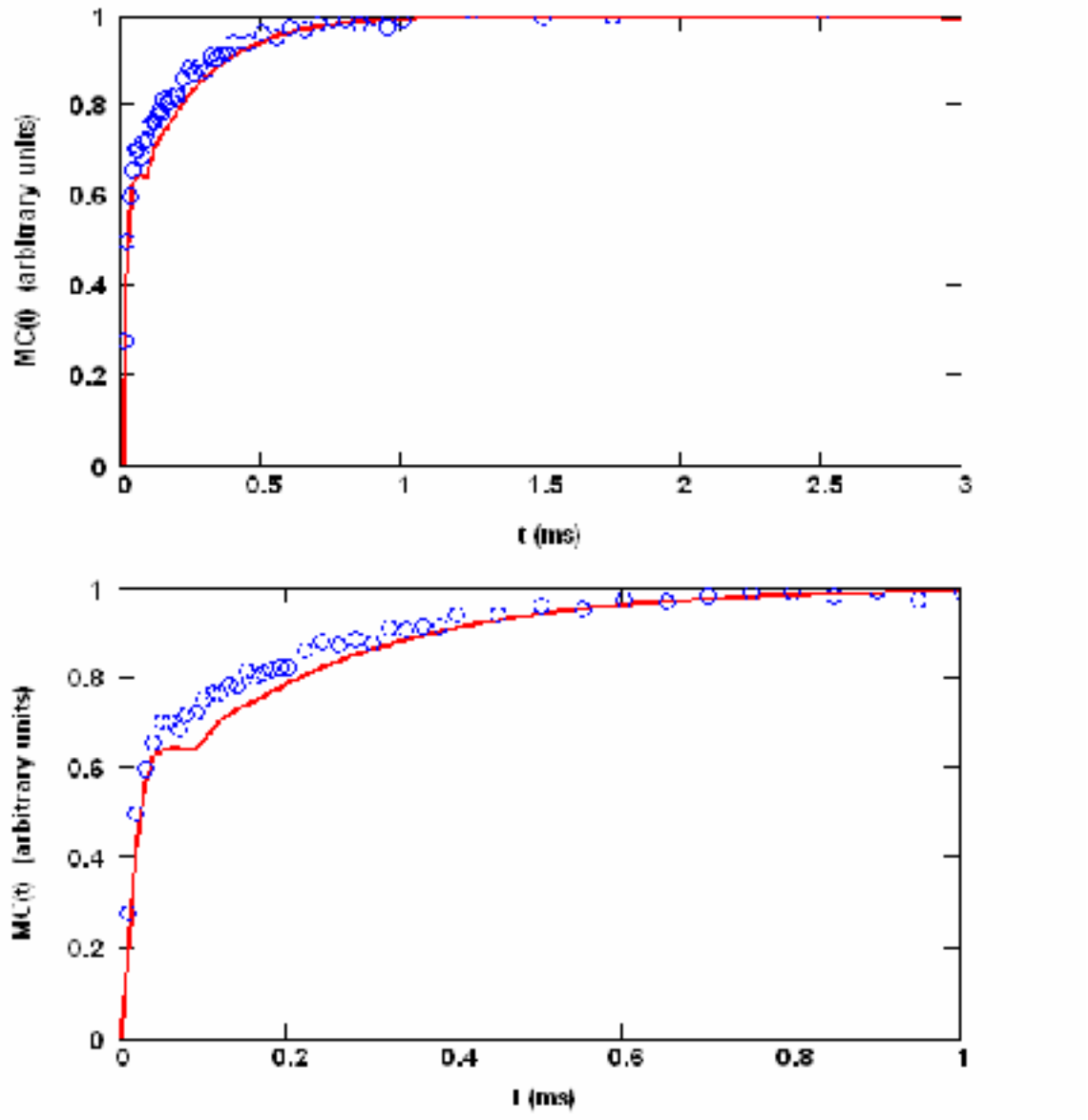

Figure 9. ^{13}C CP/MAS variable-contact data for the 59.7-ppm resonance of polycrystalline sucrose. The sample was spinning at 5 kHz.

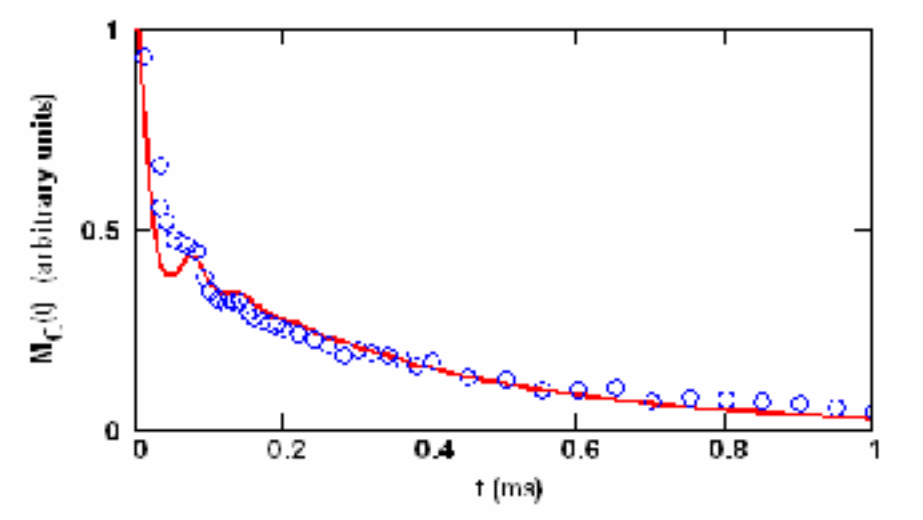

Figure 10. Carbon magnetization as a function of depolarization time in a ^{13}C CP/MAS depolarization experiment on the methylene resonance of α-glycine. The sample was spinning at 5 kHz. The solid line is a fit of equation (3) to the data.

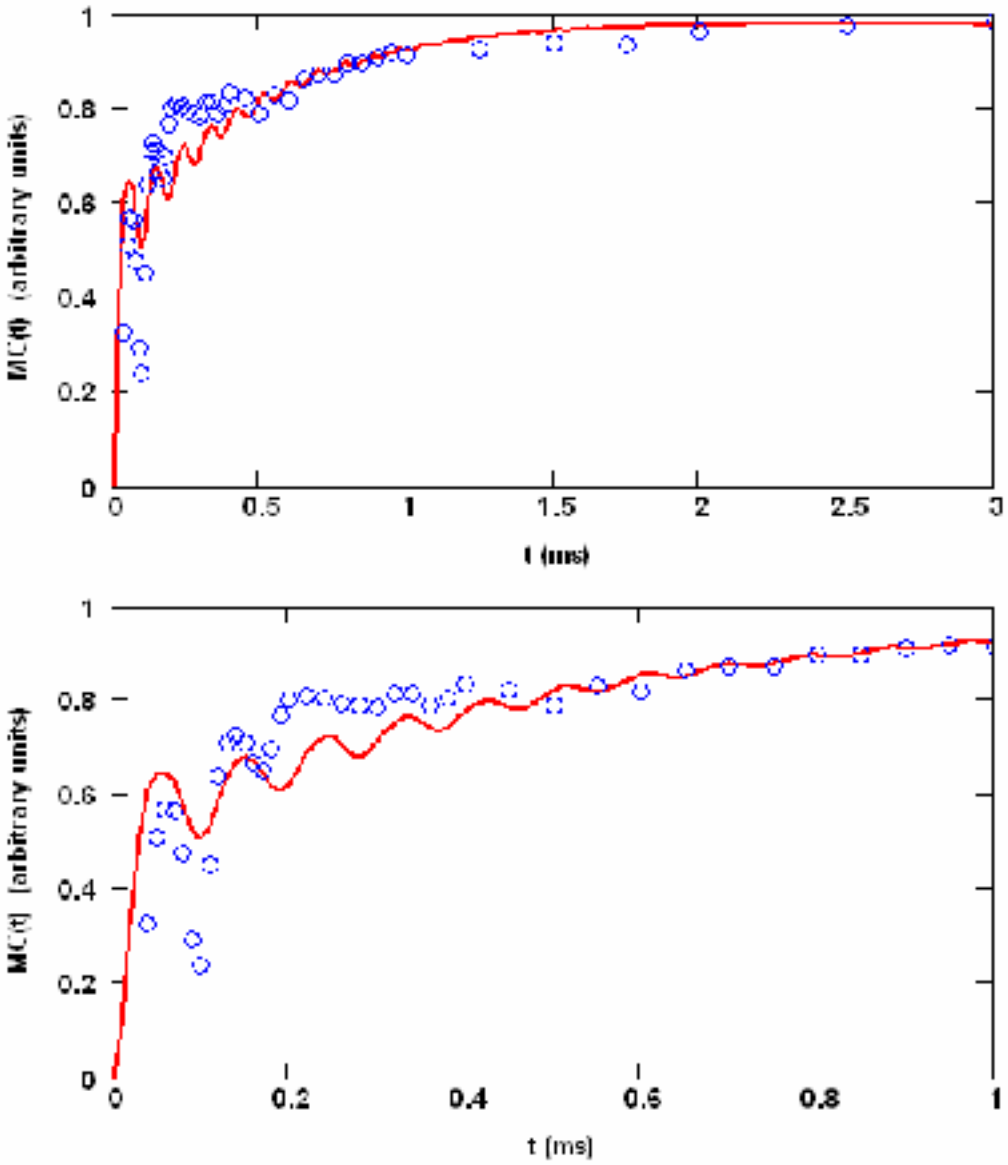

Figure 11. ^{13}C CP/MAS variable-contact data for the methylene resonance of α-glycine at a spinning speed of 13 kHz.

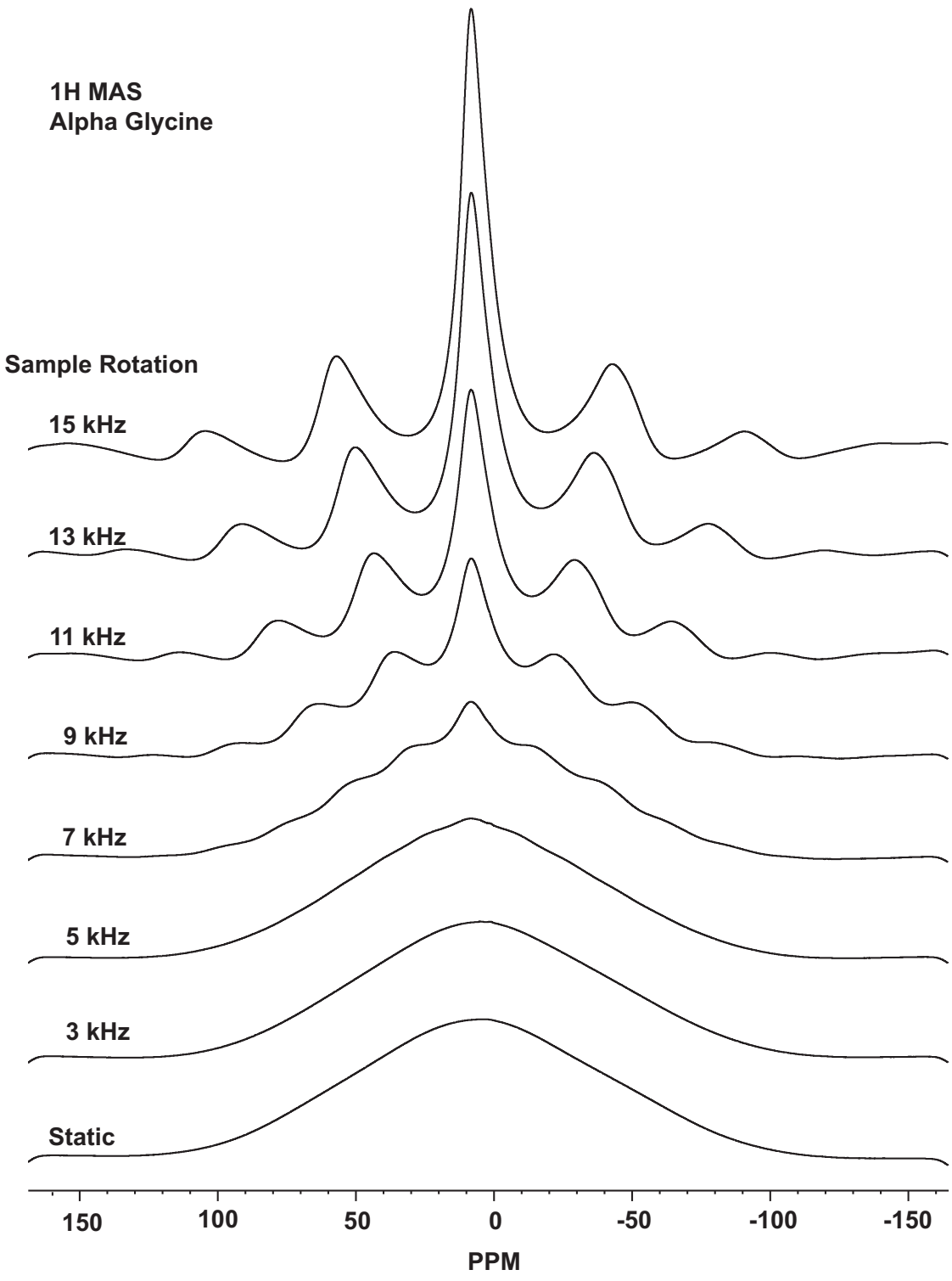

Figure 12. ^{1}H NMR spectra of α-glycine as a function of sample rotation speed.

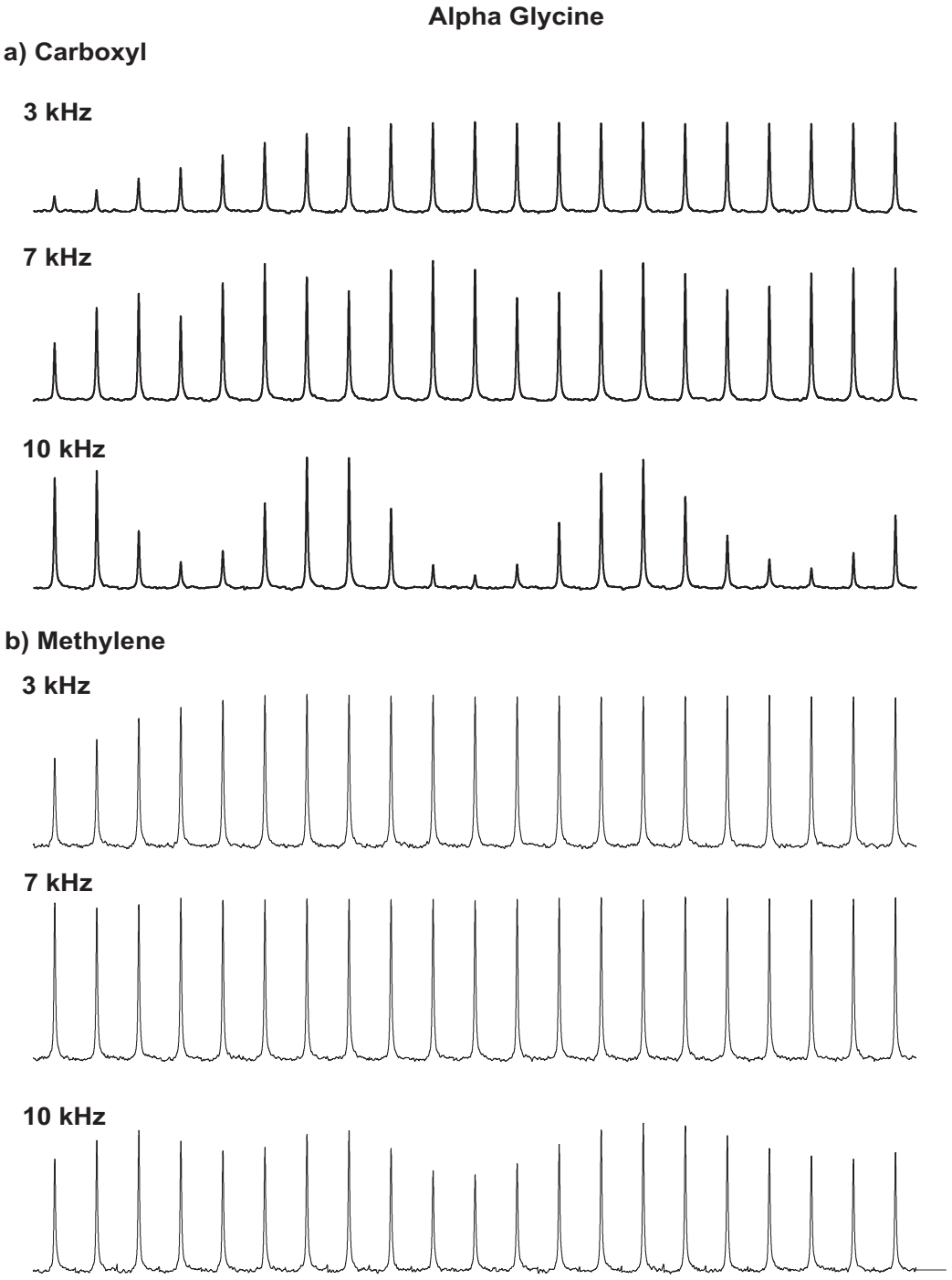

Figure 13. ^{13}C intensities of α-glycine as a function of the CP/MAS Hartmann-Hahn match for 3 ms, showing the effect of ^{13}C RF power. The power level of the first experiment on the left is 11.7 dB, and each subsequent level from left to right is incremented by 0.2 dB. The upper three traces show the carboxyl resonance at spinning rates of 3, 7, and 10 kHz as the ^{13}C RF power is incremented. The bottom three traces show the results for the methylene resonance at the same three spinning rates.

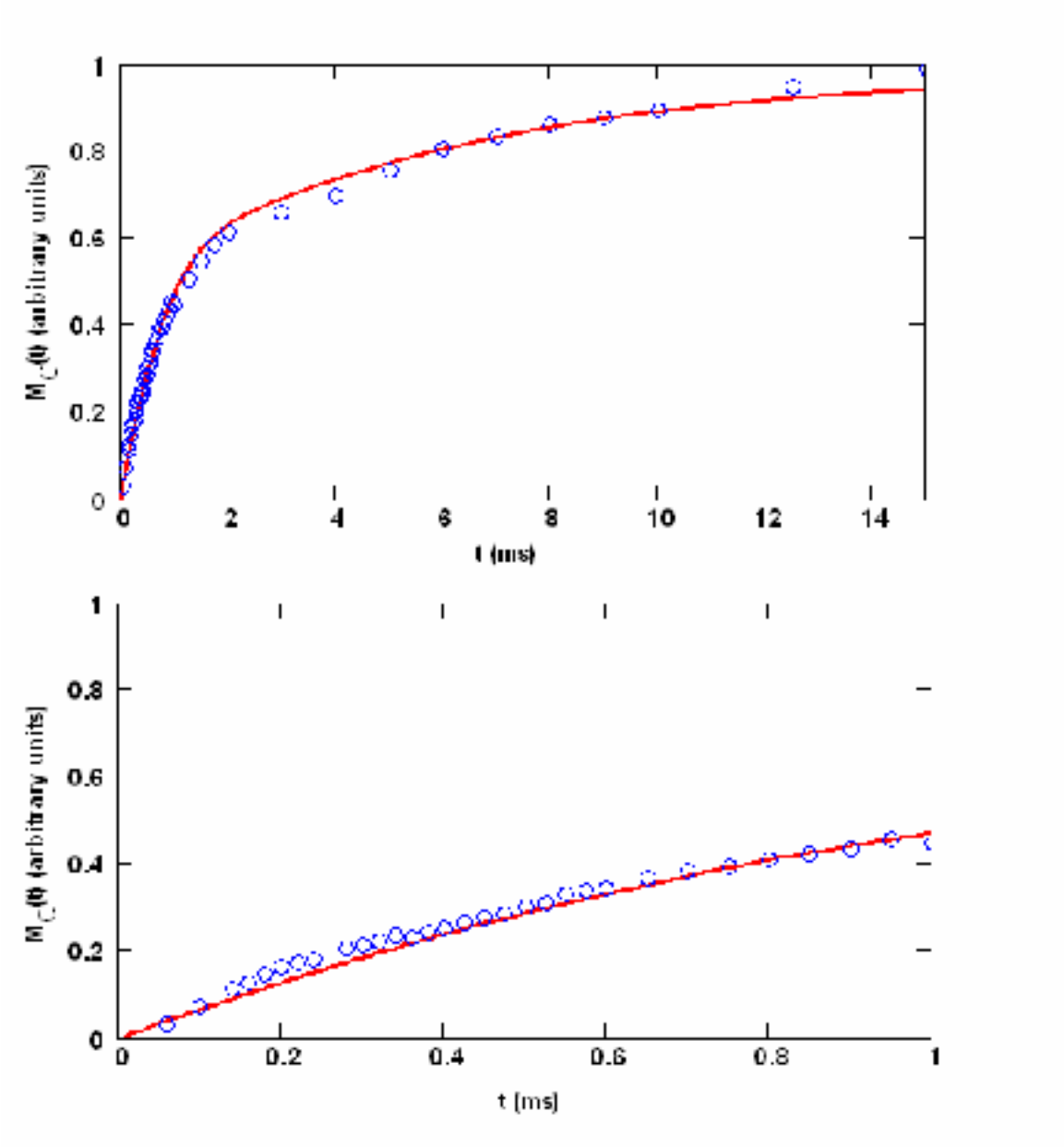

Figure 14. ^{13}C CP variable-contact data for the methylene resonance of a static sample of adamantane. The solid lines represent a fit to equation (1). The bottom panel is an expansion of the first one millisecond of transfer.